JACS
JOURNAL OF THE AMERICAN CHEMICAL SOCIETY

COMMUNICATION

pubs.acs.org/JACS

Iridium(III) Complex-Coated Nanosystem for Ratiometric Upconversion Luminescence Bioimaging of Cyanide Anions

Jinliang Liu,[†] Yi Liu,[†] Qian Liu,[†] Chunyan Li,[†] Lining Sun,[‡] and Fuyou Li*[,†]

[†]Department of Chemistry, Fudan University, 220 Handan Road, Shanghai 200433, P. R. China

[‡]Research Center of Nano Science and Technology, Shanghai University, Shanghai 200444, P. R. China

Supporting Information

ABSTRACT: Chromophoric iridium(III) complex-coated $NaYF_4$: 20%Yb, 1.6%Er, 0.4%Tm nanocrystals are demonstrated as a ratiometric upconversion luminescence (UCL) probe for highly selective detection of cyanide anion and bioimaging of CN^- in living cells through inhibition of the energy transfer from the UCL of the nanocrystals to the absorbance of the chromophoric complex. The UCL probe provides a very low detection limit of 0.18 μM CN^- in the aqueous solution.

Cyanide is well-known as a hazardous chemical in biology and the environment, and is extremely toxic to mammals.[1] Cyanide poisoning can lead to vomiting, loss of consciousness, and eventual death. According to the World Health Organization, the maximum acceptable level of cyanide in drinking water is 1.9 μM.[2] Consequently, there is considerable interest in selective detecting aqueous cyanide at sub-micromolar concentrations by using simple and visualized methods.[3−6]

Fluorescent chemodosimeters based on specific chemical reactions always show better selectivity,[7] and some of them with detection limit of sub-micromole cyanide anion were achieved in organic solvents.[5,6] However, when water was added in these systems, the response reactions become difficult and need a several hundred-fold excess of cyanide anions, longer time, or the use of elevated reaction temperature to speed up the reaction.[6a] How to avoid the negative effect of water on specific cyanide reaction becomes a challenge for highly sensitive sensing cyanide in the aqueous solution. When the reactant is bonded on the surface of one nanoparticle, its interface reaction will be affected by its surround condition. Thus, interface reaction on the nanoparticles surface provides one possible strategy to improve the sensing sensitivity.

To further develop the possible applications of fluorescent chemodosimeters of CN^- in biosystems, near-infrared (NIR) light instead of UV and visible light becomes a more suitable excitation source, because NIR light penetrates deeper into tissues and has less damage to biosamples.[8] Recently, Yoon et al. have reported one example of NIR fluorescence imaging of CN^-.[7] Compared with fluorescence imaging, upconversion luminescence (UCL) imaging based on rare-earth upconversion nanophosphors (UCNPs)[9−12] as probe has been proved to exhibit no autofluorescence (noise) from biosamples and deeper penetration depth.[13] In the present study, upconversion $NaYF_4$: 20%Yb, 1.6%Er, 0.4%Tm nanocrystals (UCNPs) were combined into a CN^- responsive chromophoric complex Ir1. Interestingly, after co-coating a hydrophobic oleic acid (OA) as co-ligand, the resulting upconversion nanosystem (denoted as OA-Ir1-UCNPs, see Scheme 1) shows highly sensitive UCL sensing CN^- in the aqueous solution and bioimaging of CN^- in living cells, upon the irradiation of NIR light at 980 nm.

Scheme 1. Proposed Recognition Mechanism and the FRET Process of OA-Ir1-UCNPs towards CN^-

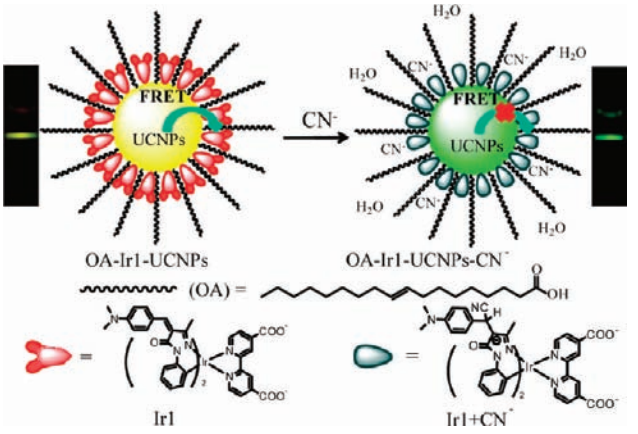

Ratiometric luminescent measurements permit signal rationing, and thus provide built-in correction for environmental effects. The design strategy of this probe is based on CN^- modulating the Förster resonance energy transfer (FRET) process[14] in OA-Ir1-UCNPs, with ratiometric UCL emission as the output signal. To this end, $NaYF_4$: 20%Yb, 1.6%Er, 0.4% Tm nanocrystals with visible UCL were used as energy donor, with NIR UCL emission at 800 nm as internal standard; meanwhile, a CN^- responsive and chromophoric iridium complex (Ir1, Scheme 1) was chosen as energy acceptor. To obtain a relative hydrophobic surrounding for Ir1, some oleic acids (OA) were also coated on the surface of UCNPs to construct one nanosystem, OA-Ir1-UCNPs. In the absence of CN^-, Ir1 shows a significant absorbance with the maximum at 505 nm (full width of half-maximum is ~70 nm) and a molar extinction coefficient of 10^5 M^{-1} cm^{-1} (Figure 1), corresponding to significant spectral overlap between the green UCL of UCNPs and the absorption of Ir1 (Figure 1). As a result, FRET occurs, and a ratio (I_{540}/I_{800}) of UCL intensity at 540 and 800 nm is weak. In the presence of CN^-, reaction of CN^- with the α,β-unsaturated

Received: June 24, 2011
Published: September 05, 2011

ACS Publications © 2011 American Chemical Society

dx.doi.org/10.1021/ja205907y | J. Am. Chem. Soc. 2011, 133, 15276–15279

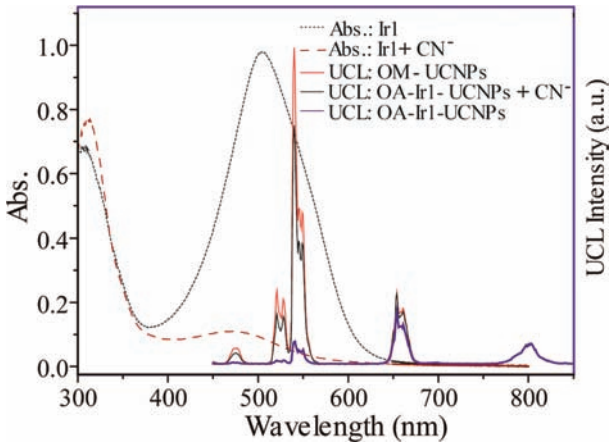

Figure 1. UV/vis absorption and photoluminescence spectra of Ir1, OM-UCNPs, and OA-Ir1-UCNPs upon addition of CN^-.

carbonyl ligand induces weak absorption in the visible region, corresponding to low spectral overlap between the absorption of Ir1 and the green UCL. Therefore, FRET is suppressed, and the ratio I_{540}/I_{800} is enhanced.

Complex Ir1 can be used to selectively detect CN^- over other anions. Only addition of CN^- causes a drastic bleaching of the absorbance peaked at 505 nm and a color change from pink to colorless (Figure S1). The absorbance intensity bleached linearly with the CN^- concentration in the range 0−20 equiv, and the reaction reached saturation when 30 equiv CN^- had been added (Figure S2). Further ^{1}H NMR and ESI-MS investigation indicated that the reaction of Ir1 with CN^- involved strong chemical addition of CN^- to an α,β-unsaturated carbonyl moiety,[5d] leading to disruption of the π-conjugation system (Figures S4−S6), which is in agreement with the observation by Bian and Huang et al.[5d] By virtue of its extremely large ε ($\log \varepsilon = 5.0$), the detection limit of Ir1 was estimated to be 1.73 μM (Figure S3a).

The OA-Ir1-UCNPs were well-dispersed and uniform with an average diameter of 20 nm, and no aggregates were observed in the TEM images (Figure 2b,c). The XRD pattern of OA-Ir1-UCNPs shows that the diffraction lines are ascribed to the hexagonal structure of $NaYF_4$ (JCPDS No.16-0334) (Figure 2d). In the FTIR spectrum of OA-Ir1-UCNPs (Figure S7), the appearance of some new peaks attributable to Ir1 suggested the successful coating of Ir1 onto the surface of UCNPs. The simultaneous observation of Ir, Y, Yb, and F in XPS analysis also indicated that Ir1 had been combined with the UCNPs (Figure S8). Moreover, negligible Ir1 was cleaved from the UCNPs even when OA-Ir1-UCNPs was stored in water for 1 month. In addition, the Ir complex content of the OA-Ir1-UCNPs was determined as 7.4 wt % (Figure S9) by a UV/vis absorption technique. Together with the result from TG analysis, we noted that the OA on the surface of the UCNPs was ~8 wt % (Figure S10). These results suggested that each UCNPs nanoparticle was coated with ~500 Ir1 molecules, and the ratio of OA and Ir1 on the surface of OA-Ir1-UCNPs was approximately 2:1.

Under CW excitation at 980 nm, the OA-Ir1-UCNPs shows four UCL emission bands at 514−534, 534−560, 635−680, and 800 nm, attributable to the $^2H_{11/2} \rightarrow {}^4I_{15/2}$, $^4S_{3/2} \rightarrow {}^4I_{15/2}$, and $^4F_{9/2} \rightarrow {}^4I_{15/2}$ transitions of Er^{3+} and $^3H_4 \rightarrow {}^3H_6$ transition of Tm^{3+}, respectively.[9b] The integral of the UCL intensities at the 635−680 nm band is approximately 2-fold of that at 514−560 nm, leading to a yellow UCL color (Scheme 1). By normalizing

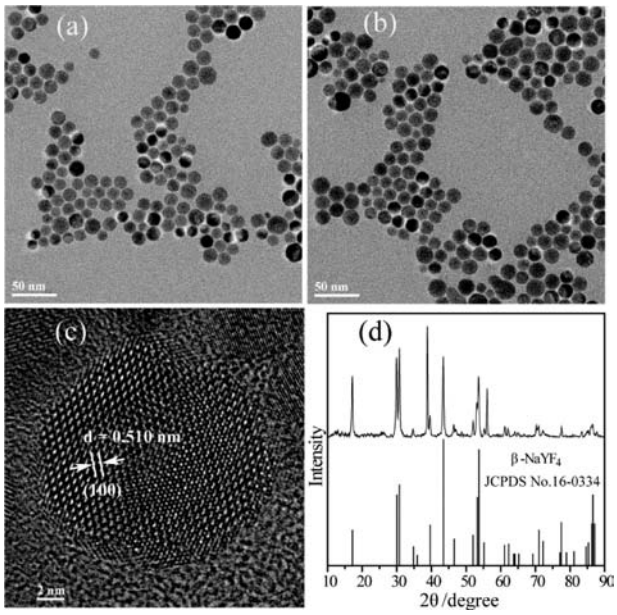

Figure 2. TEM images of OM-UCNPs (a) and OA-Ir1-UCNPs (b), HR-TEM image of OA-Ir1-UCNPs (c), and X-ray diffraction patterns of $NaYF_4$: 20%Yb, 1.6%Er, 0.4%Tm (d).

UCL at 800 nm, the OA-Ir1-UCNPs display weaker UCL at 514−560 nm than OM-UCNPs do (Figure 1), which may be attributed to FRET from the green UCL of UCNPs to the pink absorbance of Ir1, with an efficiency of ~70%.

Upon addition of CN^- to a solution of OA-Ir1-UCNPs, a color change from pink to colorless was observed, and the green UCL emission was enhanced, accompanied with the appearance of a new UCL emission at 475 nm (corresponding to the $^1G_4 \rightarrow {}^3H_6$ transition of Tm^{3+}). Detailed absorption and UCL titrations of OA-Ir1-UCNPs containing 10 μM Ir1 with various concentrations of CN^- (0−50 equiv) are shown in Figure 3. The absorbance intensity bleached linearly with the CN^- concentration in the range 0−10 equiv, and the reaction reached saturation when 15 equiv of CN^- were added, corresponding to a drastic color change from pink to colorless (Figure 4a). The detection limit was measured to be 0.95 μM. Compared with the detection limit of 1.73 μM for the free complex Ir1, the detection limit of OA-Ir1-UCNPs was evidently improved. This may occur becaue the hydrophobic OA co-ligands envelop complex Ir1 and thus improve the reaction sensitivity. Meanwhile, the intensity of the green UCL emission at 514−560 nm increased linearly with the CN^- concentration in the range 0−10 equiv, and the reaction reached saturation upon addition of 15 equiv of CN^-. Interestingly, when the UCL emission at 800 nm was used as an internal standard, and the ratio I_{540}/I_{800} was chosen as the detection signal, the detection limit of the OA-Ir1-UCNPs was estimated to be 0.18 μM. Such a low detection limit can be attributed to the ratiometric detection and a low fluorescence background for UCL detection. In addition, the time-dependent absorption changes of Ir1 and OA-Ir1-UCNPs in the presence of excess cyanide anions (40 equiv) show the reaction of OA-Ir1-UCNPs was even faster than that of Ir1 (Figure S11). Although OA-Ir1-UCNPs cannot function in purely aqueous media, such a low detection limit of 0.18 μM suggests that a solution of OA-Ir1-UCNPs in DMF may be mixed with drinking water to determine whether the level of CN^- therein exceeds 1.9 μM (the World Health Organization).

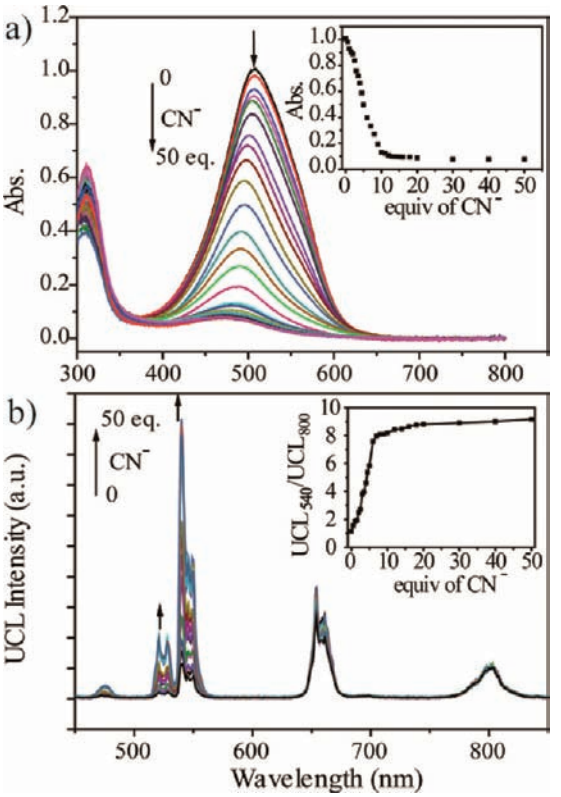

Figure 3. Changes in absorption spectra (a) and UCL spectra (b) of 10 μM OA-Ir1-UCNPs in DMF/H_2O (9:1, v/v) upon addition of CN^-. Inset: the absorbance at 505 nm (a) and the ratio (I_{540}/I_{800}) of UCL intensities at 540 and 800 nm (b) of OA-Ir1-UCNPs as a function of CN^- concentration. Excitation by CW 980 nm laser with a power density of 45 W cm^{-2}.

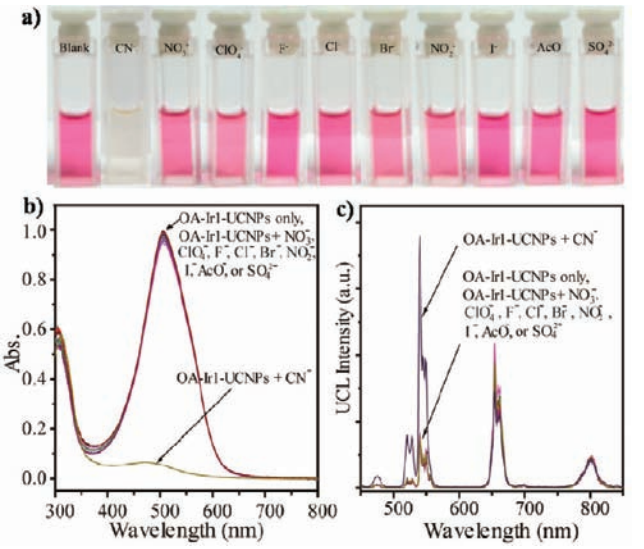

Figure 4. The photos of color changes (a) of the OA-Ir1-UCNPs upon addition of various anions, and absorption spectra (b) and UCL spectra (c) of OA-Ir1-UCNPs (10 μM) in DMF/H2O (9:1, v/v) solution upon addition of 1 mM of different anions.

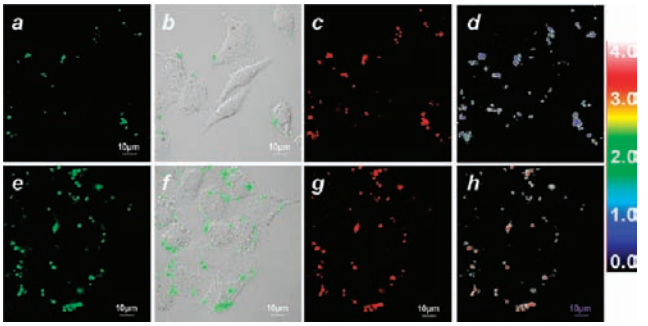

Figure 5. Ratiometric UCL images in HeLa cells (top, a-d) and 50 μM CN^- pretreated Hela Cells (bottom, e-h) incubated with 5 μM OA-Ir1-UCNPs for 2 h at 37 °C. Emission was collected by green UCL channel from 515−560 nm (a and e) and red channel from 635−680 nm (c and g). (d and h) Ratiometric UCL images with ratio function with green channel and red channel; (b and f) overlay of brightfield imaging and green UCL imaging (λ_{ex} = 980 nm).

The possibility of achieving high selectivity for CN^- over other potentially competing species was investigated. As shown in Figure 4, only the addition of CN^- led to drastic absorbance bleaching and enhancement of the green UCL emission of the UCNPs, and no significant color changes were observed in experiments using other anions, such as NO_3^-, ClO_4^-, F^-, Cl^-, Br^-, NO_2^-, I^-, AcO^-, and SO_4^{2-}, indicating that OA-Ir1-UCNPs can selectively detect CN^- over other anions. The high selectivity of this probe is attributed to the unique reaction of CN^- with the α,β-unsaturated carbonyl moiety, leading to the disruption of the π-conjugation system. In the competition experiments, CN^- was added to the solutions containing OA-Ir1-UCNPs and these anions mentioned above. These co-existent ions had negligible interfering effect on the sensing of CN^- by OA-Ir1-UCNPs in solution (Figure S12). Therefore, the excellent selectivity of OA-Ir1-UCNPs to CN^- over these anions in aqueous media indicates its utility for biological applications.

The cytotoxicity of the OA-Ir1-UCNPs was evaluated on the basis of the reduction activity of methyl thiazolyl tetrazolium (MTT). The viability of untreated cells was assumed to be 100%. On the basis of sample doses, OA-Ir1-UCNPs exhibited good cell viability (Figure S13). Specifically, cell viabilities of 90% and 80% even at a high-dose concentration of 800 μg/mL were observed after 24 and 48 h, respectively. These data indicate satisfactory *in vitro* biocompatibilities at all dosages of the nanoparticles, thus, enabling the OA-Ir1-UCNPs to serve as a potential probe for UCL imaging.

Furthermore, laser-scanning upconversion luminescence microscopy (LSUCLM)[13a] experiments were carried out to demonstrate the applicability of the OA-Ir1-UCNPs in the bioimaging of intracellular CN^- (Figure 5). As determined by LSUCLM, HeLa cells incubated with OA-Ir1-UCNPs (5 μM) for 1 h at 37 °C showed only a weak UCL emission at 515−560 nm (Figure 5a). When the cells were supplemented with 50 μM CN^- in the growth medium for 20 h at 37 °C and then incubated with OA-Ir1-UCNPs under the same conditions, a significant enhancement of the green UCL emission was observed in the intracellular region (Figure 5e). Brightfield measurements with or without treatment with CN^- confirmed that the cells remained viable throughout the imaging experiments. Overlay of UCL imaging and brightfield images revealed that the UCL signals were localized in the cytosol region (Figure 5f), indicating the subcellular distribution of CN^-.

Furthermore, in light of the rapid enhancement of green UCL at 515−560 nm over red UCL at 635−680 nm under excitation

of UCNPs with 980 nm light (Figure 3b), the ratiometric UCL imaging was investigated when UCL emissions were collected at green channel (515−560 nm) and red channel (635−680 nm). As shown in Figure 5d, HeLa cells incubated with 5 μM OA-Ir1-UCNPs for 2 h at 37 °C showed a ratio of the green UCL channel to red one of <1. Upon incubation with 5 μM OA-Ir1-UCNPs to CN^- pretreated HeLa cells, however, the ratio of green UCL to red one was increased to be ~3 (Figure 5h). The results suggest that OA-Ir1-UCNPs could be used for monitoring intracellular CN^- with ratiometric UCL methods.

In summary, we have developed chromophoric iridium(III) complex-coated $NaYF_4$: 20%Yb, 1.6%Er, 0.4%Tm nanocrystals and have demonstrated their utility as a ratiometric UCL probe for bioimaging of cyanide anion in living cells. Through inhibition of the FRET process from the UCL emission of the nanocrystals to the absorbance of the chromophoric iridium complex, the OA-Ir1-UCNPs nanosystem can be used as a ratiometric UCL probe for highly selective detection of CN^- over other anions. The low detection limit of 0.18 μM CN^- makes OA-Ir1-UCNPs practically applicable for detecting CN^- in drinking water. Furthermore, by means of LSUCLM experiments, the OA-Ir1-UCNPs nanosystem can be used as a ratiometric UCL probe for monitoring CN^- in living cells. To the best of our knowledge, this is the first example of a ratiometric UCL probe for both sensing and bioimaging of an anion. The results provide a useful design strategy of new ratiometric UCL probes for low-molecular-weight species (such as metal ions and anions) in living cells

■ ASSOCIATED CONTENT

Supporting Information. Experimental details and additional characterization. This material is available free of charge via the Internet at http://pubs.acs.org.

■ AUTHOR INFORMATION

Corresponding Author
fyli@fudan.edu.cn

■ ACKNOWLEDGMENT

The authors greatly acknowledge the financial support from NSFC (20825101, 21001072, and 91027004), NHTPC (2011AA03A407), Shanghai Sci. Tech. Comm. (11XD1400200, and 1052nm03400), IRT0911, SLADP (B108).

■ REFERENCES

(1) Panda, M.; Robinson, N. C. *Biochemistry* **1995**, *34*, 10009.
(2) Shan, D.; Mousty, C.; Cosnier, S. *Anal. Chem.* **2004**, *76*, 178.
(3) Xu, Z.; Chen, X.; Kim, H. N.; Yoon, J. *Chem. Soc. Rev.* **2010**, *39*, 127.
(4) (a) Ros-Lis, J. V.; Martinez-Manez, R.; Soto, J. *Chem. Commun.* **2002**, 2248. (b) Tomasulo, M.; Raymo, F. M. *Org. Lett.* **2005**, *7*, 4633. (c) Chen, C. L.; Chen, Y. H.; Chen, C. Y.; Sun, S. S. *Org. Lett.* **2006**, *8*, 5053. (d) Palomares, E.; Martinez-Diaz, M. V.; Torres, T.; Coronado, E. *Adv. Funct. Mater.* **2006**, *16*, 1166. (e) Yang, Y. K.; Tae, J. *Org. Lett.* **2006**, *8*, 5721. (f) Hong, S. J.; Yoo, J.; Kim, S. H.; Kim, J. S.; Yoon, J.; Lee, C. H. *Chem. Commun.* **2009**, 189. (g) Dai, Z.; Boon, E. M. *J. Am. Chem. Soc.* **2010**, *132*, 11496.
(5) (a) Kim, G. J.; Kim, H. J. *Tetrahedron Lett.* **2010**, *51*, 185. (b) Lee, J. H.; Jeong, A. R.; Shin, I. S.; Kim, H. J.; Hong, J. I. *Org. Lett.* **2010**, *12*, 764. (c) Park, S.; Kim, H. J. *Chem. Commun.* **2010**, *46*, 9197. (d) Lou, B.; Chen, Z. Q.; Bian, Z. Q.; Huang, C. H. *New J. Chem.* **2010**, *34*, 132.
(6) (a) Lee, K. S.; Kim, H. J.; Kim, G. H.; Shin, I.; Hong, J. I. *Org. Lett.* **2008**, *10*, 49. (b) Chung, S. Y.; Nam, S. W.; Lim, J.; Park., S.; Yoon, J. *Chem. Commun.* **2009**, 2866. (c) Chen, X. Q.; Nam, S. W.; Kim, G. H.; Song, N.; Jeong, Y.; Shin, I.; Kim, S. K.; Kim, J.; Park, S.; Yoon, J. *Chem. Commun.* **2010**, *46*, 8953.
(7) (a) Liu, B.; Tian, H. *Chem. Commun.* **2005**, 3156. (b) Ning, Z. J.; Chen, Z.; Zhang, Q.; Yan, Y. L.; Qian, S. X.; Cao, Y.; Tian, H. *Adv. Funct. Mater.* **2007**, *17*, 3799. (c) Zhao, Q.; Li, F. Y.; Huang, C. H. *Chem. Soc. Rev.* **2010**, *39*, 3007.
(8) Guo, Z. Q.; Zhu, W. H.; Zhu, M. M.; Wu, X. M.; Tian, H. *Chem.—Eur. J.* **2010**, *16*, 14424.
(9) (a) Wang, F.; Liu, X. G. *Chem. Soc. Rev.* **2009**, *38*, 976. (b) Wang, G. F.; Peng, Q.; Li, Y. D. *Acc. Chem. Res.* **2011**, *44*, 322.
(10) (a) Wang, F.; Han, Y.; Lim, C. S.; Lu, Y. H.; Wang, J.; Xu, J.; Chen, H. Y.; Zhang, C.; Hong, M. H.; Liu, X. G. *Nature* **2010**, *463*, 1061. (b) Wang, F.; Liu, X. G. *J. Am. Chem. Soc.* **2008**, *130*, 5642. (c) Schafer, H.; Ptacek, P.; Eickmeier, H.; Haase, M. *Adv. Funct. Mater.* **2009**, *19*, 3091. (d) Bogdan, N.; Vetrone, F.; Ozin, G. A.; Capobianco, J. A. *Nano Lett.* **2011**, *11*, 835. (e) Boyer, J. C.; Vetrone, F.; Cuccia, L. A.; Capobianco, J. A. *J. Am. Chem. Soc.* **2006**, *128*, 7444. (f) Abel, K. A.; Boyer, J. C.; van Veggel, F. C. J. M. *J. Am. Chem. Soc.* **2009**, *131*, 14644. (g) Sivakumar, S.; van Veggel, F. C. J. M.; May, P. S. *J. Am. Chem. Soc.* **2007**, *129*, 620. (h) Wang, G. F.; Peng, Q.; Li, Y. D. *J. Am. Chem. Soc.* **2009**, *131*, 14200. (i) Mai, H. X.; Zhang, Y. W.; Si, R.; Yan, Z. G.; Sun, L. D.; You, L. P.; Yan, C. H. *J. Am. Chem. Soc.* **2006**, *128*, 6426. (j) Carling, C. J.; Boyer, J. C.; Branda, N. R. *J. Am. Chem. Soc.* **2009**, *131*, 10838.
(11) (a) Achatz, D. E.; Meier, R. J.; Fischer, L. H.; Wolfbeis, O. S. *Angew. Chem., Int. Ed.* **2011**, *50*, 260. (b) Fischer, L. H.; Harms, G. S.; Wolfbeis, O. S. *Angew. Chem., Int. Ed.* **2011**, *50*, 4546. (c) Li, Z. Q.; Zhang, Y.; Jiang, S. *Adv. Mater.* **2008**, *20*, 4765. (d) Nyk, M.; Kumar, R.; Ohulchanskyy, T. Y.; Bergey, E. J.; Prasad, P. N. *Nano Lett.* **2008**, *8*, 3834. (e) Wu, S. W.; Han, G.; Milliron, D. J.; Aloni, S.; Altoe, V.; Talapin, D. V.; Cohen, B. E.; Schuck, P. J. *Proc. Natl. Acad. Sci. U.S.A.* **2009**, *106*, 10917. (f) Kobayashi, H.; Kosaka, N.; Ogawa, M.; Morgan, N. Y.; Smith, P. D.; Murray, C. B.; Ye, X. C.; Collins, J.; Kumar, G. A.; Bell, H.; Choyke, P. L. *J. Mater. Chem.* **2009**, *19*, 6481.
(12) (a) Chen, Z. G.; Chen, H. L.; Hu, H.; Yu, M. X.; Li, F. Y.; Zhang, Q.; Zhou, Z. G.; Yi, T.; Huang, C. H. *J. Am. Chem. Soc.* **2008**, *130*, 3023. (b) Xiong, L. Q.; Yang, T. S.; Yang, Y.; Xu, C. J.; Li, F. Y. *Biomaterials* **2010**, *31*, 7078.
(13) (a) Yu, M. X.; Li, F. Y.; Chen, Z. G.; Hu, H.; Zhan, C.; Yang, H.; Huang, C. *Anal. Chem.* **2009**, *81*, 930. (b) Xiong, L. Q.; Chen, Z. G.; Tian, Q. W.; Cao, T. Y.; Xu, C. J.; Li, F. Y. *Anal. Chem.* **2009**, *81*, 8687. (c) Wang, C.; Chen, L.; Liu, Z. *Biomaterials* **2010**, *32*, 1110.
(14) Bednarkiewicz, A.; Nyk, M.; Samoc, M.; Strek, W. *J. Phys. Chem. C* **2010**, *114*, 17535.